



ELSEVIER

Journal of Molecular Catalysis B: Enzymatic 4 (1998) 33–39

 JOURNAL OF  
MOLECULAR  
CATALYSIS  
B: ENZYMATICAL

# Identification of *o*-phenylenediamine polymerization product catalyzed by cytochrome *c*

Yimin Zhu<sup>1</sup>, Jinghong Li, Zhiming Liu, Guangjin Cheng, Shaojun Dong<sup>\*</sup>,  
Erkang Wang

Laboratory of Electroanalytical Chemistry, Changchun Institute of Applied Chemistry, Chinese Academy of Sciences, Changchun, Jilin 130022, PR China

Received 25 April 1997; accepted 2 June 1997

## Abstract

The hydrogen peroxide (H<sub>2</sub>O<sub>2</sub>) and cytochrome *c*-dependent oxidation of *o*-phenylenediamine (*o*-PD) was investigated by spectrophotometry and electrochemistry. The results indicated that *o*-PD underwent facile catalytic oxidation in the presence of cytochrome *c*, and that the degradation of cytochrome *c* by hydrogen peroxide can also be partly prevented in the presence of *o*-PD. The hydroxyl radical scavengers (mannitol and sodium benzoate) and oxo-heme species scavenger (uric acid) do not inhibit the oxidation, which implies that the hydroxylation of *o*-PD may not be involved in its oxidation. Combining with the results of the mass spectrum, elemental analysis, nuclear magnetic resonance and Fourier transform infrared spectrum of the isolated product, a conceivable structure of the product was suggested. © 1998 Elsevier Science B.V.

**Keywords:** Cytochrome *c*; *o*-Phenylenediamine; Hydrogen peroxide; *o*-Phenylenediamine oxidation; Product identification

## 1. Introduction

Hemoproteins are widespread in nature and have many crucial biological roles. All hemoproteins have iron protoporphyrin IX or one of its derivatives (heme) as their prosthetic group, though their functions and reactivities vary widely. The three main functions of hemoproteins are the transport and storage of oxygen (hemoglobin and myoglobin, respectively), the transport of electrons (e.g., cytochrome *c* and

cytochrome *b*<sub>5</sub>), and the oxidation of substrates (e.g., horseradish peroxidase (HRP), cytochrome *P*-450) [1].

The variety of functions of hemoproteins stems from differences in the way the apoprotein interacts with the heme and with potential substrates. The mechanisms by which the apoprotein controls the intrinsic reactivity of the heme are of both theoretical and practical interest, so do the mechanisms by which the apoprotein interacts with substrates.

HRP catalyzes the H<sub>2</sub>O<sub>2</sub>-dependent oxidation and polymerization of substrates. *o*-phenylenediamine (*o*-PD) is a general substrate for the enzymatic reaction about HRP. In a study of HRP activity with H<sub>2</sub>O<sub>2</sub> and *o*-PD as the sub-

<sup>\*</sup> Corresponding author. Fax (86-431) 568-5653; e-mail: dongsj@sun.ihep.ac.cn

<sup>1</sup> Present address: Jilin Institute of Technology, Changchun, Jilin 130012, China.

strate, Gallati and Brodbeck [2] assumed that the 2,2'-diaminoazobenzene was the resulting product. Furthermore, Tarcha et al. [3] reported that the product of the oxidation of *o*-PD by H<sub>2</sub>O<sub>2</sub>, catalyzed by HRP, was 2,3-diaminophenazine. There are conflicting results on the reaction products from the oxidation of *o*-PD.

Recently it has been reported that cytochrome *c* catalyzes the oxidation of various electron donors in the presence of H<sub>2</sub>O<sub>2</sub>, including 2,2'-azino-bis(3-ethylbenzthiazoline-6-sulfonic acid), 4-aminoantipyrine, and luminol [4], *o*-methoxyphenol [1], lipid [5], as well as *N,N*-dimethylaniline [6]. These oxidative reactivities are so-called peroxidase activities. Considering the fact that cytochrome *c* displays the peroxidase activities, we put our attention to utilizing cytochrome *c* to catalyze the H<sub>2</sub>O<sub>2</sub>-dependent oxidation of *o*-PD. The result indicates that *o*-PD is converted to one trimer with ca. 100% selectivity.

## 2. Experimental

### 2.1. Materials

Cytochrome *c* (horse heart) from Sigma was used without further purification. H<sub>2</sub>O<sub>2</sub> (30%) from Beijing Chemicals was quantified by the titration method using KMnO<sub>4</sub> and by spectrophotometer with an absorption coefficient of 43.6 M<sup>-1</sup> cm<sup>-1</sup> at 240 nm [7,8]. 4*S*,4'*S*'-dithiopyridine (PySSPy) was obtained from Nakaral Chemicals. *o*-Phenylenediamine, mannitol, sodium benzoate and uric acid were of analytical grade. All reagents used were of the highest grade commercially available. All solutions were prepared in 0.1 M phosphate buffer (pH 6.8) and purged with high purity argon. All experiments were carried out at room temperature (18 ± 1°C).

### 2.2. Instrument

UV-vis spectrometric studies were carried out with a Tracor Northern TN-6500 rapid scan

spectrophotometer (Middleton, WI) using 1 cm light path quartz cuvette. Electrochemical experiments were performed using a PARC model 173 potentiostat and a model 175 universal programmer (EG and G PARC, Princeton, MA, USA). Cyclic voltammograms (CVs) were recorded on a Gould 60000 recorder. The electrochemical cell was a three-electrode system, the PySSPy modified gold electrode was used as a working electrode for protecting cytochrome *c* denaturation on the electrode [9], a platinum foil as an auxiliary electrode, and an Ag/AgCl (saturated KCl) as a reference electrode. The potential of this reference electrode is +200 mV versus the standard hydrogen electrode (SHE). All potentials are stated versus an Ag/AgCl electrode. Analysis of the samples was performed on a Gilson gradient HPLC system (Gilson Medical Electronics) consisting of dual pumps and a Gilson 117 UV detector at 254 nm. The column used was a reverse-phase C<sub>18</sub> column (4.0 mm × 200 mm i.d., 7 μm particle size) at a flow rate of 0.5 ml/min. The mobile phase was 50% methanol and 50% water. The mass spectrum was run on a LDI 1700-MALDI-TOF-MS. A BIO-RAD FTS-7 model fourier transform IR (FTIR) spectrometer was used to record FTIR spectra, and a KBr pellet was used as a window. Nuclear magnetic resonance (NMR) spectra were run on a Varian Unity-400 Mhz spectrometer. spectra were obtained at room temperature from solutions of samples in methanol using tetramethylsilane as an internal standard.

## 3. Results and discussion

### 3.1. UV-vis spectrometric and electrochemical measurement of H<sub>2</sub>O<sub>2</sub>-dependent oxidation of *o*-PD catalyzed by cytochrome *c*

The spectrum of the mixture solution of 9.6 μM ferricytochrome *c* and 0.417 mM *o*-PD exhibited that ferricytochrome *c* was reduced by *o*-PD (Fig. 1A). The characteristic absorption bands of the reduced cytochrome *c* were

obtained at 550, 520 and 414 nm. The magnitude of reduction of cytochrome *c* increased with concentration of *o*-PD. The results were similar to those of catechol [10].

After adding 4.0 mM H<sub>2</sub>O<sub>2</sub> into the bulk solution containing *o*-PD and cytochrome *c* and incubating for 2 min, a new absorption band appeared around 470 nm. Meanwhile cytochrome *c* was oxidized by H<sub>2</sub>O<sub>2</sub> to exhibit the characteristic absorption bands of ferricytochrome *c* at 530 nm (shown in Fig. 1B). After the above solution was incubated for 10 min, the absorption peak around 470 nm increased obviously (shown in Fig. 1C). As the final concentration of H<sub>2</sub>O<sub>2</sub> was increased to 0.018 M, the absorption band around 470 nm increasing rapidly (shown in Fig. 1D). In this time, the absorption bands of cytochrome *c* at 530 nm were still observable, the solet band of cytochrome *c* overlapped with the new absorption band at a maximum of 470 nm. It has been known that cytochrome *c* can be degraded by H<sub>2</sub>O<sub>2</sub> and hydroperoxides, with irreversible spectral changes [11] and that a rapid bleaching reaction occurred immediately after mixing cytochrome *c* with H<sub>2</sub>O<sub>2</sub> [12]. The above results exhibited that the degradation of cytochrome *c* might be partly prevented in the presence of

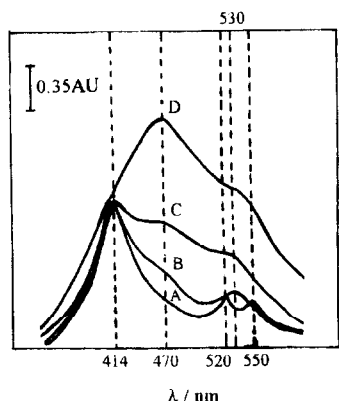


Fig. 1. UV-visible spectra for the H<sub>2</sub>O<sub>2</sub>-dependent oxidation of *o*-phenylenediamine catalyzed by cytochrome *c*. (A) Reaction mixture contained 9.6 μM cytochrome *c* and 0.417 mM *o*-phenylenediamine in 0.1 M phosphate buffer (pH 6.8). (B) Adding 4.0 mM H<sub>2</sub>O<sub>2</sub> into the (A) solution and incubating for 2 min. (C) Incubating for 10 min. (D) The final concentration of H<sub>2</sub>O<sub>2</sub>, 0.018 M, incubating for 5 min.

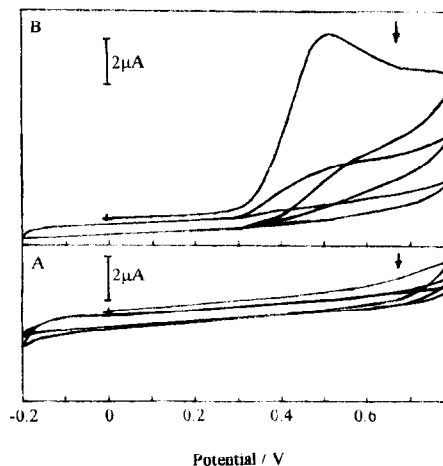


Fig. 2. Cyclic voltammograms for the oxidation of *o*-phenylenediamine. The working electrode was 4S,4S'-dithiodipyridine modified electrode. The potential scan rate was 100 mV/s. All solutions contained 0.1 M phosphate buffer (pH 6.8). (A) 0.417 mM *o*-phenylenediamine with 9.6 μM cytochrome *c* and 4.0 mM H<sub>2</sub>O<sub>2</sub>; (B) 0.417 mM *o*-phenylenediamine. The potential was successively swept.

*o*-PD and its oxidation product. In the absence of cytochrome *c*, the compared experiment for H<sub>2</sub>O<sub>2</sub>-dependent oxidation of *o*-PD did not exhibit the absorption band around 470 nm. The results suggested that cytochrome *c* catalyzed the H<sub>2</sub>O<sub>2</sub>-dependent oxidation of *o*-PD, and that a stable product absorbing at 470 nm accumulated.

The H<sub>2</sub>O<sub>2</sub>-dependent oxidation of *o*-PD catalyzed by cytochrome *c*, was measured by using CV, as shown in Fig. 2A. No obvious CV peak can be observed. It had been widely accepted that the PySSPy modified gold electrode had the most effective promotion for cytochrome *c* in solution, and showing a reversible one-electron transfer process of the native protein [9]. Since no observable redox peak current was obtained in the range of the applied potential (Fig. 2A), it is possible that the PySSPy modified gold electrode surface was changed in the experimental condition. The CV of *o*-PD alone showed an irreversible anodic peak at about +0.5 V, and on successive scans the peak current dropped significantly with each scan until ultimately no current flowed (shown in Fig. 2B). This indi-

cated that a self-insulating electropolymerization film to form on electrode surface [13]. In neutral solution, the study on the polymer structure has seldom been reported. Because cytochrome *c* catalyzed the  $H_2O_2$ -dependent oxidation of *o*-PD, *o*-PD and the product covered or adsorbed on the electrode surface and may further polymerize to insulate the electrode. Thus Fig. 2A exhibited a nonconducting film characteristic.

### 3.2. Effect of scavengers of the active oxygen on $H_2O_2$ -dependent oxidation of *o*-PD

Cytochrome *c* and other hemoproteins react with  $H_2O_2$  to form a species as a hydroxyl radical or an oxo-heme complex ( $Fe^{4+}=O$ ) [4,14,15]. To estimate if active oxygen species participating in  $H_2O_2$ -dependent oxidation of *o*-PD, a variety of scavengers had been added into the *o*-PD–cytochrome *c*– $H_2O_2$  system. The hydroxyl radical scavengers [14], mannitol and sodium benzoate at an excess concentration (0.1 M) seldom effected the oxidation of *o*-PD. Since UV–visible spectra did not significantly change. Uric acid was an excellent scavenger of the oxo-heme species [14]. But no inhibition by uric acid ruled out the possibility of the oxo-heme species to be the oxidative agent also.

In general, cytochrome *c* can interact with  $H_2O_2$ , giving rise to hydroxyl radicals [11]. When cytochrome *c* reacted with  $H_2O_2$  it was proposed that a bound hydroxyl radical [11,14] formed by a site-specific reaction at the heme or activation of cytochrome *c* by  $H_2O_2$  to a catalytically active species, a high oxidation state of an oxo-heme complex [14], mediated the hydroxylation of substrates. In these cases, the hemoprotein was degraded and bleached by  $H_2O_2$  with the apparent disappearance of the characteristic absorption bands for heme in the protein, which suggested that iron ions released or mobilized from the protein reacted with  $H_2O_2$  to form the reactive species ( $OH^\cdot$ ,  $Fe^{3+}-OH^\cdot$  or  $Fe^{4+}=O$ ) [11,12,14]. But the absorption spectra in Fig. 1 of the reaction mixtures indicated

incomplete destruction of heme. Spectrophotometric results also showed that  $H_2O_2$  can not significantly oxidize *o*-PD in the absence of cytochrome *c*. While cytochrome *c* reduction observed with *o*-PD suggested an out-sphere mechanism similar to catechol [10], with the heme edges as the most likely site for electron donation. Thus, in the *o*-PD–cytochrome *c*– $H_2O_2$  system, it was possible that  $H_2O_2$  can oxidize *o*-PD located at the heme edges. Furthermore, *o*-PD and its oxidized species may partly prevent from degradation of cytochrome *c*. In addition, it may be considered in which  $H_2O_2$ -dependent oxidation of *o*-PD did not involve the hydroxylation of *o*-PD, i.e. the oxygen element was not involved in the product of *o*-PD oxidation.

### 3.3. Preparation of the product of $H_2O_2$ -dependent oxidation of *o*-PD

For the purpose of identifying the structure of the product, preparative incubations of 50 ml contained 0.1 M potassium phosphate (pH 6.8), *o*-PD (2.0 g, 11 mmol), and  $H_2O_2$  (2.0 ml, 30%) in a round-bottom flask equipped with a magnetic stirrer. The flask was chilled in an ice bath to approximately 10°C and cytochrome *c* (20 mg), dissolved in distilled water (1.0 ml), was added. After 15 min the ice bath was removed and the reaction was allowed to con-

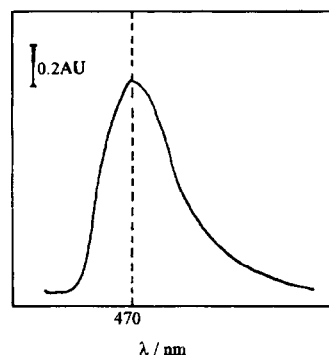


Fig. 3. UV–visible spectrum for the isolated product of  $H_2O_2$ -dependent oxidation of *o*-phenylenediamine. The solution contained 0.11 mM of the isolated product in 0.1 M phosphate buffer (pH 6.8).

tinue for 20 h. The precipitate which had formed was isolated by filtration and recrystallized from dioxane/benzene giving the pure product (0.5 g, yield 25%). Fig. 3 shows the visible spectrum of the isolated product in 0.1 M phosphate buffer (pH 6.8). An absorption band with a maximum at 470 nm can be observed, which is consistent with that in Fig. 1.

### 3.4. HPLC analysis

Fig. 4 shows the HPLC separation of UV-absorbing *o*-PD metabolites from H<sub>2</sub>O<sub>2</sub> and cytochrome *c*-catalyzed reaction mixtures. Under the conditions used in these experiments, the retention times of *o*-PD (I) and the product (II) were approximately 6.82 and 12.96 min, respectively. These elution patterns of the compounds correspond exactly with the retention times of *o*-PD and the above isolated product injected as

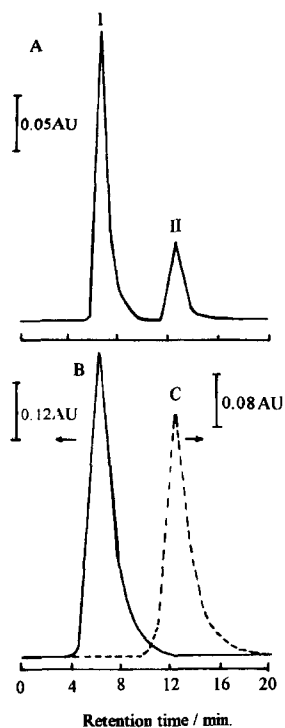


Fig. 4. (A) Chromatogram obtained from the incubation of 0.417 mM *o*-phenylenediamine with 4.0 mM H<sub>2</sub>O<sub>2</sub> and 9.6 μM cytochrome *c*; (B) for *o*-phenylenediamine; (C) for the isolated product of *o*-phenylenediamine.

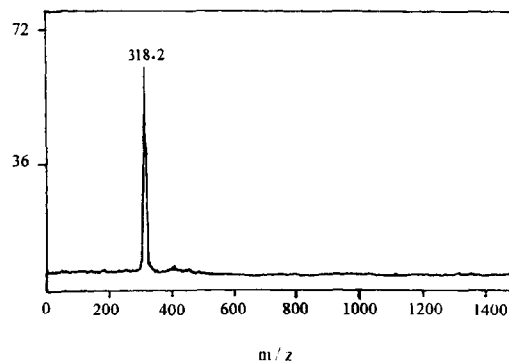


Fig. 5. Mass spectrum of the isolated product of *o*-phenylenediamine.

methanol solutions. The HPLC analysis of the resulting product solution shows the presence of the peak (II) as the only product.

### 3.5. Structure characterization of the isolated product

Mass spectrometry (MS) was used for molecular weight determination of the isolated product. As shown in Fig. 5, MS analysis of the isolated product indicated molecular ion consistent with the formation of one trimer ( $M_r$  318.2). Elemental analysis suggested a molecular formula, C<sub>18</sub>H<sub>18</sub>N<sub>6</sub> (Calc.: C, 67.92; H, 5.66; N, 26.42%. Found: C, 67.75; H, 5.54; N, 26.31%), which corresponds to a possible molecular formula, C<sub>18</sub>H<sub>18</sub>N<sub>6</sub>. In previous studies, the results obtained by Tarcha et al. [3] indicated that the product of the oxidation of *o*-PD by H<sub>2</sub>O<sub>2</sub>, catalyzed by HRP, was 2,3-diaminophenazine, which corresponds to a formula C<sub>12</sub>H<sub>10</sub>N<sub>4</sub> ( $M_r$  210). While Gallati and Brodbeck [2] assumed that 2,2'-diaminoazobenzene was the resulting product, which corresponds to a formula C<sub>12</sub>H<sub>12</sub>N<sub>4</sub> ( $M_r$  212). These previous reports indicated the oxidation product is consistent with the formation of a dimer. But these dimers were absent from Fig. 5 and H<sub>2</sub>O<sub>2</sub> and cytochrome *c*-catalyzed oxidation of *o*-PD was obviously different from that of the HRP.

The FTIR absorption spectrum of a KBr pellet of the isolated product is shown in Fig. 6,

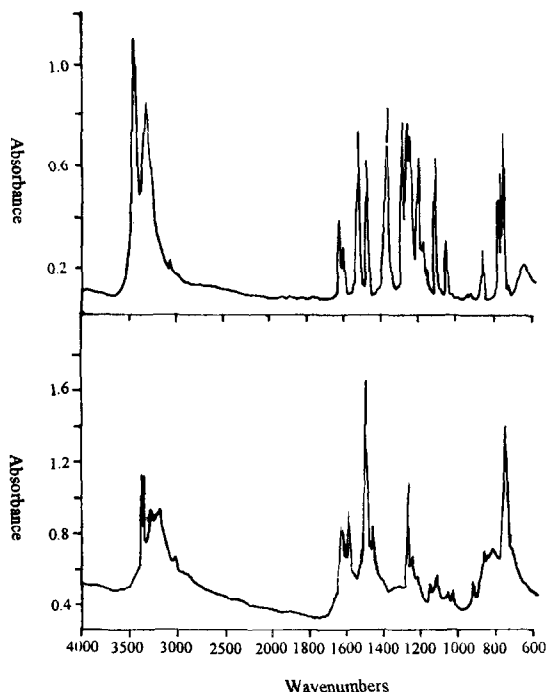


Fig. 6. FTIR absorption spectra of (A) *o*-phenylenediamine, (B) the isolated product.

together with the spectrum of *o*-PD. These spectral data are summarized in Table 1. The absorption peaks at ca. 3000 and 1450–1620  $\text{cm}^{-1}$ , which are common to the isolated product and *o*-PD, are characteristics of the stretching vibration modes of the C–H and C=C bonds, respectively, of the aromatic nuclei [16,17]. The absorption peaks due to the N–H stretching vibrations [17] of the amino groups of the isolated product and *o*-PD were observed at 3320–3450  $\text{cm}^{-1}$ , which two absorption peaks

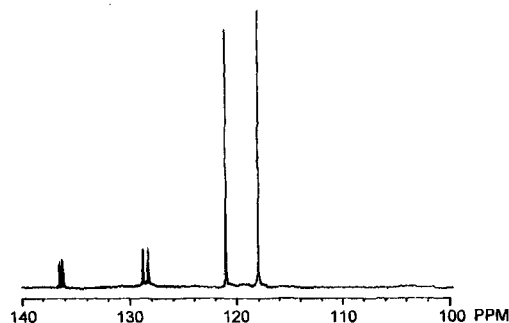


Fig. 7. Carbon-13 spectrum of the isolated product of *o*-phenylenediamine.

corresponding to the N–H stretching vibrations of the amino groups, forming hydrogen bonds [16,17], of the isolated product were observed at 3290 and 3192  $\text{cm}^{-1}$ . The absorption peaks ascribable to the stretching vibrations of C–N bonds were observed at 1220–1370  $\text{cm}^{-1}$  [16,17]. Several absorption peaks, which arise from the C–H out-of-plane bending modes [16,17], were observed for all the samples examined. For the isolated product, the peaks at 750, 870 and 927  $\text{cm}^{-1}$  can be considered to correspond to 1,2-disubstituted and 1,2,3,4-tetra-substituted benzene structures [16,17].

Carbon-13 and proton NMR spectra of the isolated product are consistent with the more symmetrical structure. Fig. 7 shows the carbon-13 spectrum, which identifies the two methine carbons of the aromatic ring (121.048 and 118.029 ppm) and the four quaternary carbons of the aromatic ring (136.502, 136.228, 128.793 and 128.353 ppm). The distortionless enhancement by polarization transfer (DEPT) pulse se-

Table 1

FTIR absorption spectra of the isolated product and *o*-phenylenediamine (fundamental vibrations)

Compound	Vibration mode					
	$\nu$ (N–H) <sup>a</sup> $\text{cm}^{-1}$	$\nu$ (C–H) <sup>b</sup> $\text{cm}^{-1}$	$\nu$ (C=C) <sup>b</sup> $\text{cm}^{-1}$	$\nu$ (C–N) <sup>c</sup> $\text{cm}^{-1}$	$\nu$ (C–H) <sup>d</sup> $\text{cm}^{-1}$	$\nu$ (C–H) <sup>e</sup> $\text{cm}^{-1}$
<i>o</i> -PD	3450, 3326	3050	1619, 1599, 1513, 1469	1363, 1280, 1255, 1241	1188, 1166, 1095, 1040	849, 769, 755, 741
Product	3383, 3361, 3290, 3192	3070	1630, 1591, 1500, 1458	1273, 1248, 1225	1155, 1117, 1057, 1031	927, 870, 821, 750

<sup>a</sup> Stretching vibration of the N–H bonds.

<sup>b</sup> Stretching vibration of the C–H and C=C bonds.

<sup>c</sup> Stretching vibration of the C–N bonds.

<sup>d</sup> Bending vibration of the C–H bonds.

<sup>e</sup> Out-of-plane bending modes of the C–H bonds.

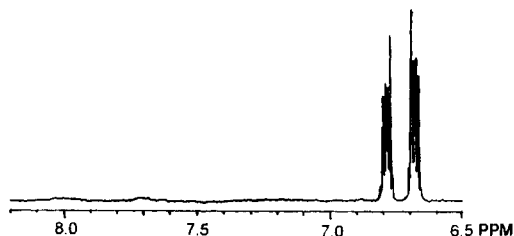
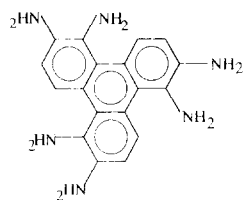


Fig. 8. Proton spectrum of the isolated product of *o*-phenylenediamine.

quence [18] confirms the two methine carbons. The aromatic proton NMR spectrum of the isolated product is shown in Fig. 8. The protons with resonances at 6.682 and 6.782 ppm are shown by proton–proton spin coupling constants to be *ortho* to one another ( $J = 6.12$  Hz) [19].

Considering the results of MS, NMR, FTIR, elemental analysis and chemical scavengers, a product structure such as Scheme 1 is conceivable. This product is named 1,2,5,6-tetra-amino-9,10-(1',2'-di-aminobenzo-)phenanthrene (*o*-PD trimer).

In conclusion, cytochrome *c* catalyzed the  $H_2O_2$ -dependent oxidation of polymerization of *o*-PD. A *o*-PD trimer was isolated from reaction mixtures. HPLC analysis of the isolated product indicated that *o*-PD was converted to the trimer with ca. 100% selectivity. The chemical structure was determined by a combination of MS, NMR, FTIR and Chemical scavengers. Obviously, the trimer is different from that of HRP and  $H_2O_2$ -dependent oxidation of *o*-PD. To gain better understanding of enzymatic oxidation mechanisms, we are extending these studies to elucidate the nature of the complexes be-



Scheme 1.

tween cytochrome *c* and *o*-PD or other similar substrates.

## Acknowledgements

The support of this project by the National Natural Science Foundation of China is greatly appreciated.

## References

- [1] A. Fujita, H. Senzu, T. Kunitake, I. Hamachi, Chem. Lett., (1994) 1219.
- [2] H. Gallati, H. Brodbeck, J. Clin. Chem. Clin. Biochem. 20 (1982) 221.
- [3] P.J. Tarcha, V.P. Chu, D. Whittern, Anal. Biochem. 165 (1987) 230.
- [4] R. Radi, L. Thomson, H. Rubbo, E. Prodanov, Arch. Biochem. Biophys. 288 (1991) 112.
- [5] R. Radi, J.F. Turrens, B.A. Freeman, Arch. Biochem. Biophys. 288 (1991) 118.
- [6] I. Hamachi, A. Fujita, T. Kunitake, J. Am. Chem. Soc. 116 (1994) 8811.
- [7] M. Louis, Handbook of Analytical Chemistry, McGraw-Hill, New York, NY, 1963.
- [8] A.G. Hildebrandt, I. Rotts, M. Tjoe, G. Heinemeyer, Methods Enzymol. 52 (1978) 34.
- [9] I. Taniguchi, K. Toyosawa, H. Yamaguchi, K. Yasukouchi, J. Chem. Soc., Chem. Commun., (1982) 1032.
- [10] M.M.M. Saleem, M.T. Wilson, Biochem. J. 201 (1982) 433.
- [11] E. Cadenas, A. Boveris, B. Chance, Biochem. J. 187 (1980) 131.
- [12] F. Xu, D.E. Hultquist, Biochem. Biophys. Res. Commun. 181 (1991) 197.
- [13] W.R. Heineman, H.J. Wieck, A.M. Yacynych, Anal. Chem. 52 (1980) 345.
- [14] Y. Zhu, J. Li, S. Dong, J. Chem. Soc., Chem. Commun., (1996) 51.
- [15] P. Barr, R.P. Mason, J. Inorg. Biochem. 59 (1995) 441.
- [16] K. Nakanishi, IR Absorption Spectroscopy, Nankodo, Tokyo, 1970.
- [17] A.D. Cross, R.A. Jones, An Introduction to Practical Infrared Spectroscopy, 3rd ed., Butterworth, London, 1969.
- [18] D.M. Doddrell, D.T. Pegg, M.R. Bendall, J. Magn. Reson. 48 (1982) 323.
- [19] L.M. Jackman, S. Sternhell, in: D.H.R. Barton, W. Doering